

Supplementary Material

A breakthrough method for the recycling of spent lithium-ion batteries without pre-sorting

Jialiang Zhang^{a,b,c}, Guoqiang Liang^{a,b}, Cheng Yang^{a,b}, Juntao Hu^{a,b}, Yongqiang Chen^{a,b,c}, Chengyan Wang^{a,b,c*}

^a State Key Laboratory of Advanced Metallurgy, University of Science and Technology Beijing, No. 30 Xueyuan Road, Haidian District, Beijing 100083, China

^b School of Metallurgical and Ecological Engineering, University of Science and Technology Beijing, No. 30 Xueyuan Road, Haidian District, Beijing 100083, China

^c Beijing Key Laboratory of Green Recycling and Extraction of Metals, No. 30 Xueyuan Road, Haidian District, Beijing 100083, China

***Corresponding author:** Tel.: 861062332271; Fax: 861062333170;

E-mail: chywang@yeah.net (C. Wang)

1 Experimental Section

1.1 Materials and reagents

The spent ternary lithium-ion batteries used in the experiment were purchased from a local company for battery recovery. The spent batteries were discharged, disassembled, and cut into pieces. The battery scraps were dissolved with aqua regia, and the content of valuable metal elements in the raw material was analyzed by inductively coupled plasma emission spectrometer (ICP-OES, Optima 7000 DV, Perkin Elmer instruments, US). The content of F was measured by ion-selective electrode method. The results of chemical composition of electrode scraps are listed in Table S1.

Table S1 Chemical composition of the spent NCM battery scraps

Element	Li	Ni	Co	Mn	Cu	Al	P	F
wt.%	3.15	13.17	5.18	6.96	13.56	7.77	2.16	2.99

1.2 Experimental procedures

Firstly, 25 g of battery scraps and the lignite (0–24.77% of battery scraps mass) with a carbon content of 62.2% were mixed at a quartz crucible and roasted in a muffle furnace at a heating rate of 10 °C/min in an air atmosphere. All the waste gas generated during the roasting process was absorbed by 1 mol/L NaOH solution. The effects of roasting temperature (500–750 °C) and carbon dosage (0–15.4%) on the leaching efficiency of Li, Ni, Co, Cu were studied at a fixed roasting time (3 h). X-ray diffractometer (XRD, RINT-TTR3, RIGAKU, Japan) at scanning angle of 10–90° was used to determine the phases of the roasted products. After reduction roasting, the

roasted product was immediately taken out and put into water for rapid cooling, then the roasted product was mixed with water and leached with the CO₂ introduction at a flow rate of 30 mL/min in a three-mouth round-bottom flask placed on a magnetic stirrer for 2 h at a liquid-solid ratio of 10 mL/g. After filtering, ICP-OES was used to analyze the content of the valuable metals in the filtrate.

After carbonation water leaching, the filtration residue was leached with NH₃·H₂O (0.3–1.2 times the mass of battery scraps) and (NH₄)₂SO₄ (1–2.5 times the mass of battery scraps) mixed solution with continuous air injection. After filtration, the content of valuable metals in the filtrate was tested by ICP-OES. The phase composition of the carbonation water leaching and ammonia leaching residues was determined by XRD. The leaching efficiency of Li, Ni, Co and Cu is calculated by Eq. (1)

$$\eta_i = \frac{c_i V_i}{m_0 w_i} \times 100\% \quad (1)$$

where c_i and V_i are the concentration of metal i and the volume of leaching solution respectively; m_0 and w_i are the mass of the electrode mixtures and the content of Li, Ni, Co and Cu in the raw materials respectively.

2 Results and Discussion

Table S2 Thermodynamic data for H₂O, NH₃, O₂, Ni and Co at 298 K and 101.3 kPa

Species	$\Delta G_f^\theta / \text{kJ} \cdot \text{mol}^{-1}$
H ₂ O	-237.14
O ₂	0
NH ₃	-26.50
NH ₄ ⁺	-79.31
Co	0
CoO	-215.18
Co(NH ₃) ₆ ²⁺	-249.81
Ni	0
NiO	-220.47
Ni(NH ₃) ₆ ²⁺	-255.84

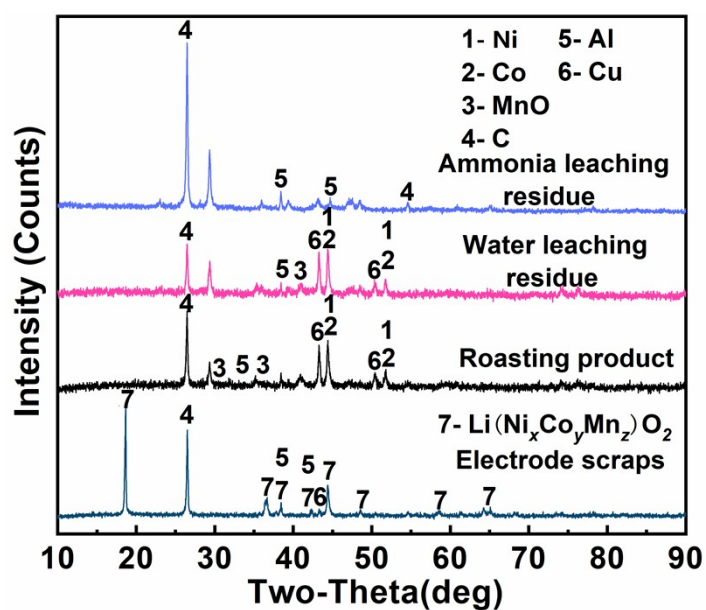


Fig.S1 XRD patterns of important intermediate products

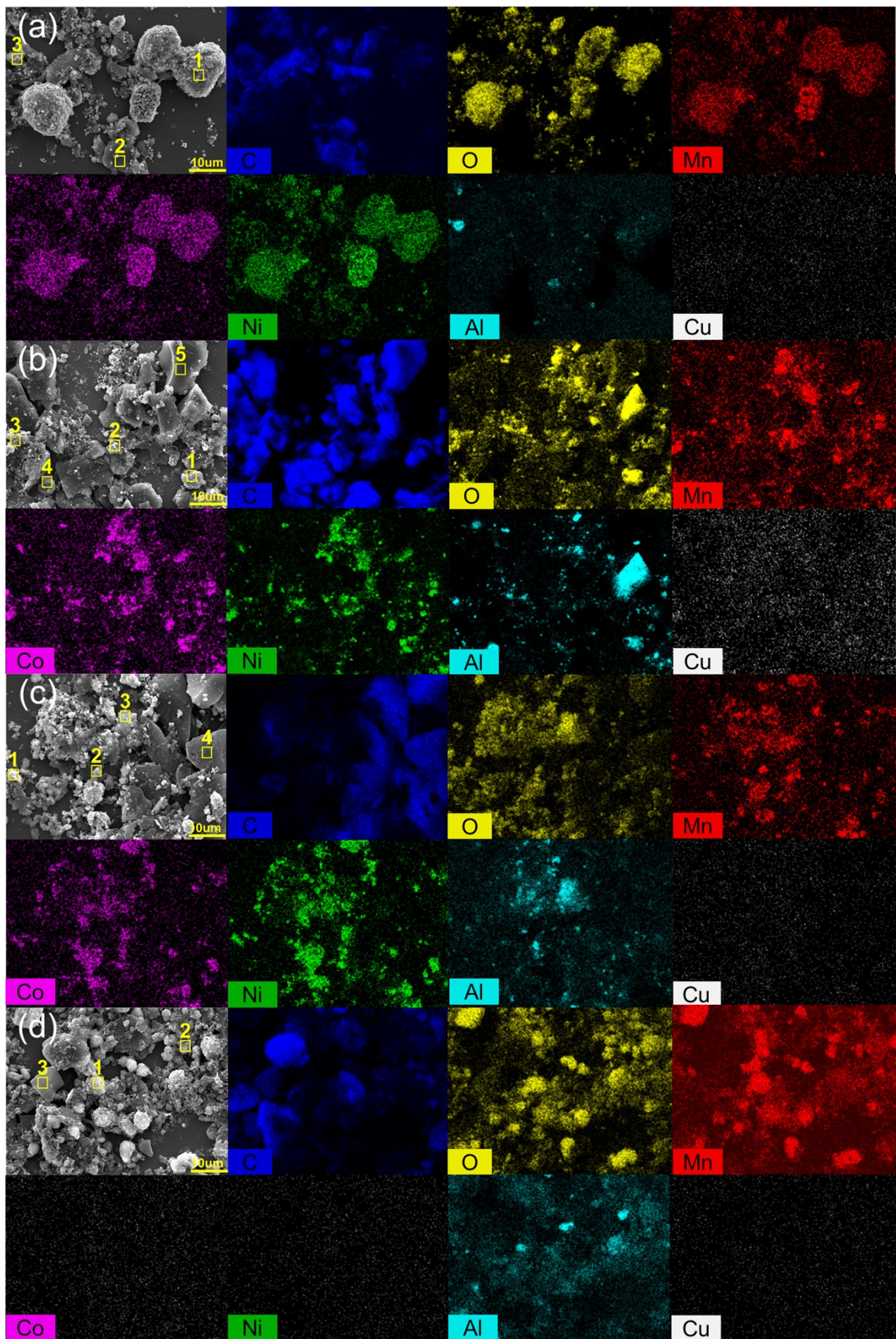


Fig.S2 SEM morphology and element distribution results of (a) electrode materials, (b)

roasting products, (c) water leaching residue and (d) ammonia leaching residue.

Table S3 EDS elemental analysis of battery material, roasting products, water leaching residue and ammonia leaching residue.

Element	Battery material			Roasting products				
	Region 1	Region 2	Region 3	Region 1	Region 2	Region 3	Region 4	Region 5
C	10.21	85.61	9.85	7.06	19.41	23.58	7.18	91.37
O	19.82	11.43	53.59	3.33	33.57	73.74	10.99	6.62
Ni	40.98	1.75	1.01	59.21	0.65	1.36	1.73	0.87
Co	14.64	0.73	0.51	23.24	0.77	0.87	0.65	0.23
Mn	13.13	0.32	0.55	5.43	43.92	0.16	0.38	0.36
Al	1.22	0.16	34.49	1.73	0.98	0.29	79.07	0.55

Element	Water leaching residue				Ammonia leaching residue		
	Region 1	Region 2	Region 3	Region 4	Region 1	Region 2	Region 3
C	11.86	15.31	29.47	92.07	18.45	31.15	70.59
O	2.85	37.52	33.79	6.57	38.25	35.41	19.32
Ni	59.39	1.86	1.58	0.51	0.35	0.72	5.44
Co	22.07	1.21	1.75	0.27	0.64	0.38	0.98
Mn	1.19	41.19	0.96	0.16	40.11	3.31	0.84
Al	2.64	2.91	32.45	0.42	1.07	29.10	2.83

Table S4 Concentration and leaching efficiency of valuable metals under optimal ammonia leaching conditions ($t=3.5$ h, ammonia dosage=48.3 g/L, L/S ratio=7.5 mL/g, $(\text{NH}_4)_2\text{SO}_4$ dosage=188.9 g/L)

Element	Concentration (g/L)	Leaching efficiency (%)
Ni	16.5	99.8
Co	6.5	95.5
Mn	0.2	1.8
Cu	18.5	95.3
Al, Fe, Ca, Mg	Trace	Trace

A 100-mesh sieve is used to screen the ammonia leaching residue to realize the separation of aluminum foil and powder containing MnO₂, graphite and etc. The separation effect of Al and Mn is shown in Table S5.

Table S5 Content of Al and Mn in oversize and undersize products (100 mesh)

Products	Al content (wt.%)	Al distribution (%)	Mn content (wt.%)	Mn distribution (%)
oversize product	80.3	82.69	2.44	3.49
undersize product	2.55	17.3	8.41	96.5

A small amount of Al in the undersize powder is removed by NaOH solution, and the removal efficiency of Al can reach 90% (liquid-solid ratio=4:1, NaOH concentration=1 mol/L, 60 °C, 1 h). Subsequently, reductive acid leaching was performed (liquid-solid ratio=3:1, H₂SO₄ concentration=1 mol/L, Na₂SO₃ dosage=twice the theoretical dosage, 60 °C, 1 h). The concentration and leaching efficiency of valuable metals in reduction acid leaching solution of the undersize powder are shown in Table S6, and the chemical composition of reduction acid leaching residue is shown in Table S7.

Table S6 Concentration and leaching efficiency of valuable metals in reduction acid leaching solution of the undersize product

Element	Mn	Co	Ni	Cu	Al
Concentration (g/L)	33.6	1.16	1.79	1.99	1.41
Leaching efficiency (%)	99.9	99.9	98.67	99.9	99.9

Table S7 Chemical composition of acid leaching residue of the undersize product

Element	Li	Al	Ni	Co	Mn	Cu	C
wt. %	0.035	0.16	0.0028	<0.001	0.006	0.035	90.2

Ni, Co and Cu in acid leaching solution are removed via sulfide precipitation with $(\text{NH}_4)_2\text{S}$ (pH=2, $(\text{NH}_4)_2\text{S}$ dosage=1.5 times the theoretical dosage, 60 °C, 2 h), and Al is removed via hydrolysis with Na_2CO_3 (liquid-solid ratio=5:1, pH=4.5, 90 °C, 1 h). The concentration of valuable metals in reduction acid leaching solution of the undersize product after purification is shown in Table S8.

Table S8 Concentration of valuable metals in reduction acid leaching solution of the undersize product after purification

Element	Ni	Co	Mn	Cu	Al
Concentration (g/L)	0.024	0.016	30.5	0.245	0

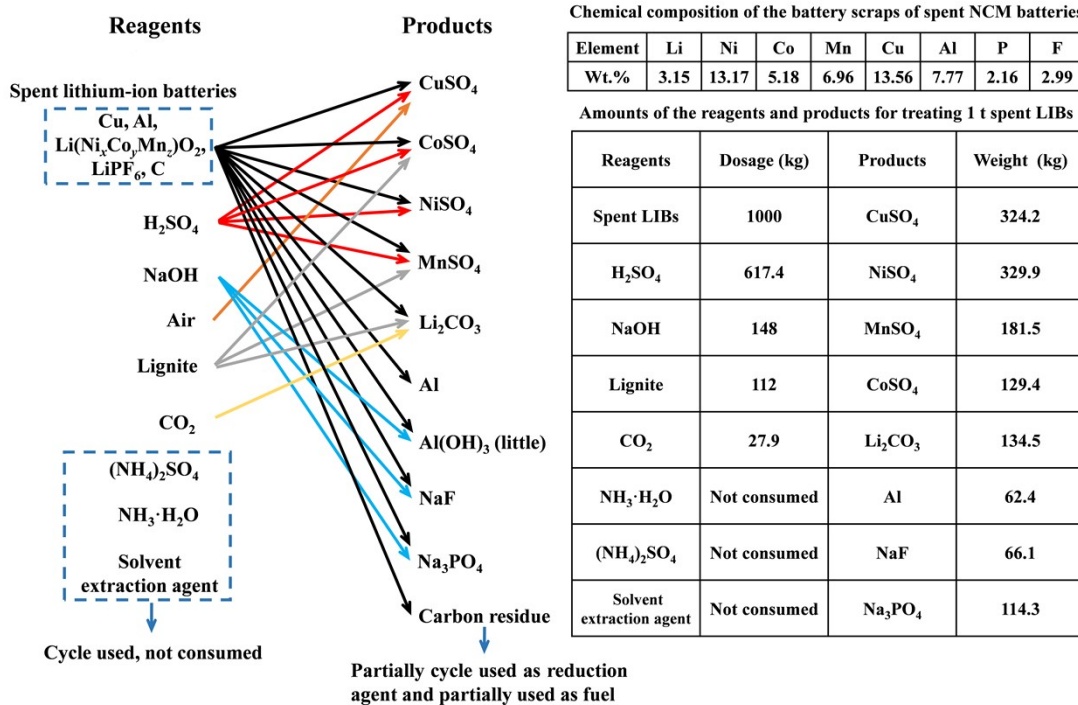


Fig.S3 Dosage of reagents, amounts of products and materials flow in the whole process

Table S9 GC-MS results of chemical composition of the gas liberated in reduction roasting process

Gas	H ₂	CO ₂	CH ₄	C ₂ H ₆	C ₃ H ₈	1, 2-C ₄ H ₆	Others
vol.%	1.33	47.79	38.16	4.72	1.39	4.72	1.89

Table S10 COD concentrations in leaching solution

Solution	Water leaching solution	Ammonia leaching solution
Concentration (g/L)	0.00452	0.1505